A time-averaged model for gas/solids flow in a one-dimensional vertical channel

Sofiane Benyahia
National Energy Technology Laboratory, Morgantown, WV 26505

Abstract

In this study, we are interested in deriving time-smoothed governing and constitutive equations for gas/solids flow in moderately-dense systems where particle-particle collision is the main dissipation mechanism. The goal of this study is to obtain a steady or time-averaged model that can be used as a reduced order model (ROM), which can then be used in process simulation software. This study is motivated by the fact that the transient gas/solids flow simulations in large-scale devices can take weeks or months to complete.

Simulation conditions

This study is conducted for a pseudo 1-D gas/solids channel flow. Both the vertical and horizontal velocity components are solved for. However, we used periodic boundary conditions with only one computational cell along the vertical or y-component; thus, all derivatives with respect to y will vanish except for the gas pressure. Traditionally, the MFIX solver used a fixed gas pressure-drop along the flow-wise, or y, direction, but it is now possible to specify a fixed gas mass flow rate and the gas pressure drop will be adjusted using Newton's algorithm to achieve the specified gas flow rate within a specified tolerance. At the walls, simple boundary conditions (BC) were used: free slip for the solids velocity and zero flux for granular temperature.

Derivation of time-averaged governing equations for gas-solids flow

The instantaneous solids continuity equation for a pseudo 1-D flow and constant solids density:

$$\frac{\partial}{\partial t}\left(\varepsilon_s\right) + \frac{\partial}{\partial x}\left(\varepsilon_s u_s\right) = 0$$

The time-averaged solids continuity is,

$$\frac{\partial}{\partial x}\left(\overline{\varepsilon_s u_s}\right) = 0$$

The Reynolds decomposition of the instantaneous variables into time-averaged and fluctuating parts:

$$\overline{\varepsilon_s u_s} = \left(\overline{\varepsilon_s} + \varepsilon_s'\right)\left(\overline{u_s} + u_s'\right) = \overline{\varepsilon_s}\,\overline{u_s} + \overline{\varepsilon_s' u_s'}$$

Thus, the continuity equation becomes:

$$\frac{\partial}{\partial x}\left(\overline{\varepsilon_s}\,\overline{u_s}\right) + \frac{\partial}{\partial x}\left(\overline{\varepsilon_s' u_s'}\right) = 0 \qquad [1]$$

The solids horizontal instantaneous momentum equation:

$$\rho_s\left[\frac{\partial}{\partial t}(\varepsilon_s u_s)+\frac{\partial}{\partial x}(\varepsilon_s u_s u_s)\right] = -\varepsilon_s\frac{\partial P_g}{\partial x}+\frac{\partial \tau_{sxx}}{\partial x}-I_{gsx}$$

Where $\frac{\partial \tau_{sxx}}{\partial x} = -\frac{\partial P_s}{\partial x}+\frac{\partial}{\partial x}\left[(\eta\mu_b+4/3\mu_s)\frac{\partial u_s}{\partial x}\right]$ and $I_{gsx}=\beta(u_s-u_g)$

Let's assume that the gas phase doesn't influence the horizontal motion of the solids; the time-averaged horizontal momentum equation becomes:

$$\rho_s\frac{\partial}{\partial x}\left[(\bar{\varepsilon}_s\bar{u}_s\bar{u}_s)+\overline{\varepsilon'_s u'_s u'_s}+\bar{\varepsilon}_s\overline{u'_s u'_s}+2\bar{u}_s\overline{\varepsilon'_s u'_s}\right] = -\frac{\partial \overline{P_s}}{\partial x}+\frac{\partial}{\partial x}\left[\overline{(\eta\mu_b+4/3\mu_s)\frac{\partial u_s}{\partial x}}\right] \qquad [2]$$

The instantaneous solids vertical (direction of flow) momentum equation:

$$\rho_s\left[\frac{\partial}{\partial t}(\varepsilon_s v_s)+\frac{\partial}{\partial x}(\varepsilon_s u_s v_s)\right] = -\varepsilon_s\frac{\partial P_g}{\partial y}+\frac{\partial \tau_{sxy}}{\partial x}-I_{gsy}-\rho_s\varepsilon_s g$$

Where $\frac{\partial \tau_{sxy}}{\partial x} = \frac{\partial}{\partial x}\left(\mu_s\frac{\partial v_s}{\partial x}\right)$ and $I_{gsy}=\beta(v_s-v_g)$

The time-averaged vertical solids momentum equation becomes:

$$\rho_s\frac{\partial}{\partial x}\left[(\bar{\varepsilon}_s\bar{u}_s\bar{v}_s)+\overline{\varepsilon'_s u'_s v'_s}+\bar{\varepsilon}_s\overline{u'_s v'_s}+\bar{u}_s\overline{\varepsilon'_s v'_s}+\bar{v}_s\overline{\varepsilon'_s u'_s}\right] = -\overline{\varepsilon_s\frac{\partial P_g}{\partial y}}+\frac{\partial}{\partial x}\left(\overline{\mu_s\frac{\partial v_s}{\partial x}}\right)-\bar{I}_{gsy}-\rho_s\bar{\varepsilon}_s g \qquad [3]$$

The instantaneous granular temperature equation:

$$\frac{3}{2}\rho_s\left[\frac{\partial \varepsilon_s\Theta_s}{\partial t}+\frac{\partial \varepsilon_s u_s\Theta_s}{\partial x}\right] = \frac{\partial}{\partial x}\left(\kappa_s\frac{\partial\Theta_s}{\partial x}\right)+\tau_{sxx}\frac{\partial u_s}{\partial x}+\tau_{sxy}\frac{\partial v_s}{\partial x}-\rho_s J_s$$

For this particular case-study, we can neglect $\tau_{sxx}\frac{\partial u_s}{\partial x}$ because of the term $\tau_{sxy}\frac{\partial v_s}{\partial x}$. Thus, the time-averaged granular temperature equation becomes:

$$\frac{3}{2}\rho_s\frac{\partial}{\partial x}\left[\bar{\varepsilon}_s\bar{u}_s\bar{\Theta}_s+\overline{\varepsilon'_s u'_s\Theta'_s}+\bar{\varepsilon}_s\overline{u'_s\Theta'_s}+\bar{u}_s\overline{\varepsilon'_s\Theta'_s}+\bar{\Theta}_s\overline{\varepsilon'_s u'_s}\right] = \frac{\partial}{\partial x}\left(\overline{\kappa_s\frac{\partial\Theta_s}{\partial x}}\right)+\overline{\mu_s\frac{\partial v_s}{\partial x}\frac{\partial v_s}{\partial x}}-\rho_s\bar{J}_s \qquad [4]$$

Apart from the gravitational force in the vertical momentum equation [3], all terms in the time-averaged gas/solids governing equations are non-linear. The convective terms yield correlations of volume fraction, the two velocity components and granular temperature. There are 9 correlations from the convective terms in this pseudo 1-D model.

Transient simulations

We first conduct transient simulations based on the instantaneous governing equations to analyze the transient behavior of the gas/solids flow. This type of simulations was conducted and details are explained by Benyahia et al. (2007). We show here transient results of flow variables at some locations in the 1-D channel.

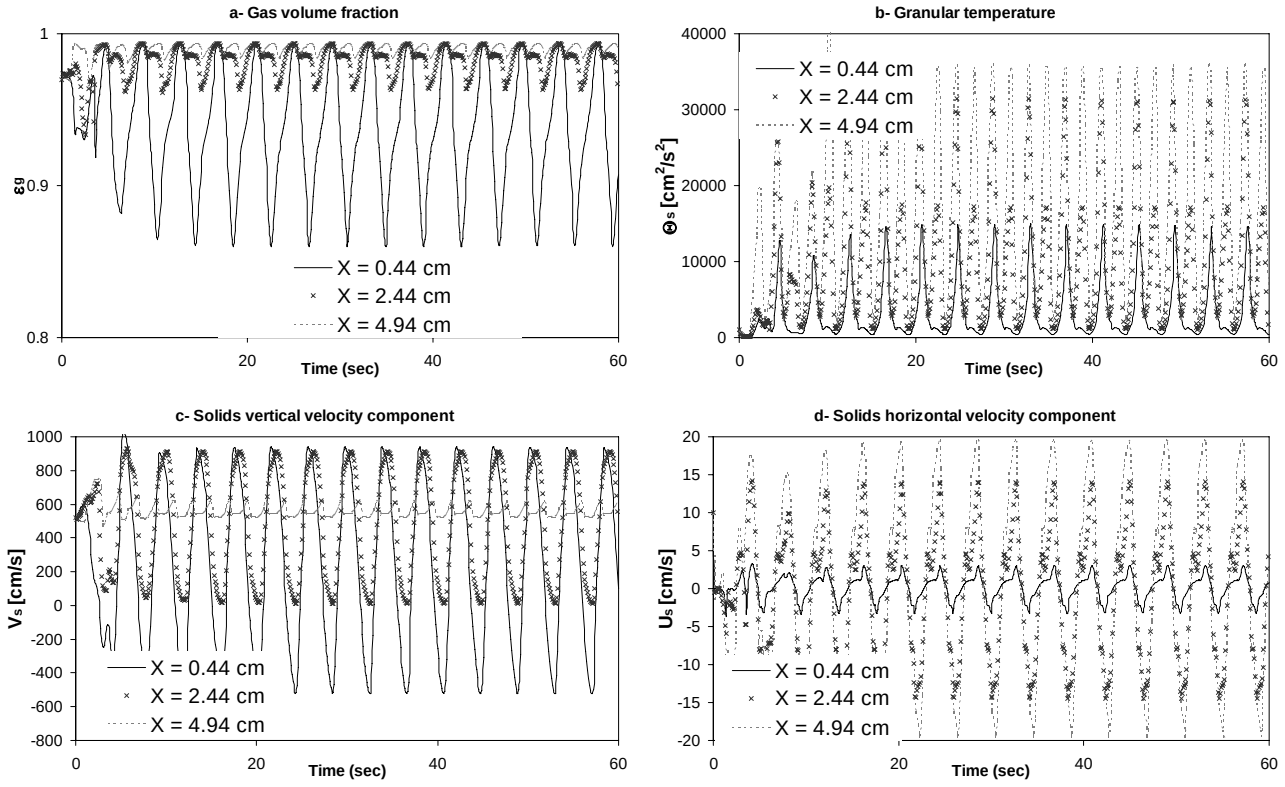

Figure 1 Transient profile of flow variables at three different locations (near the wall and at ¼ and ½ the channel width) in the 10-cm wide channel.

Figure 1 gives an idea of the large-scale fluctuations in the 1-D channel at three different locations (x=0.44 cm or near the wall, x=2.44 cm or half a distance between the center of the channel and the wall, and x=4.94 cm or the middle of the channel). An animation of the solids (or gas) volume fraction in the channel shows dense clusters of solids forming, alternatively, at one sidewall or the other in the 1-D channel. The motion of the large-scale clusters creates the oscillatory behavior observed in figure 1. After the initial transient behavior of few seconds, periodic oscillations are observed in all the flow variables at all locations. This is due to transient clusters that form periodically at one sidewall of the channel or the other. The largest deviations from the mean in the gas volume fraction and solids vertical velocity are observed near the walls of the channel where clusters form and flow downward. On the other hand, the largest amplitude of oscillation in the granular temperature is observed at the center of the channel where the flow is relatively dilute. Also the solids horizontal velocity is small near the walls because of non-penetration condition (horizontal component of solids and gas velocities are set to zero at walls) and largest deviations from the mean (zero) are observed at the center of the channel where the flow is dilute. An important fact to notice in Figure 1 is that the amplitude of the oscillations is large, so that they are not considered "fluctuations" as in single-phase flow turbulence. There is only one frequency of oscillations as the small-scale fluctuations usually observed in single-phase turbulence are not computed in this 1-D channel flow.

Constitutive relations

The constitutive relations are based on the kinetic theory for granular flow (KTGF) model derived by Gidaspow (1994). This model is similar to other "dry" granular models, such as that of Lun et al. (1984), where the dissipation of granular energy is only due to inelastic collisions. Also this model ignores corrections to the solids viscosity and conductivity for very dilute flows, which is a reasonable assumption since this study involves a moderately dense flow. These simplifications make it easier to analyze the non-linear constitutive relations derived from kinetic theory because of their dependence on solids volume fraction and granular temperature only.
The constitutive relations derived from kinetic theory are the following:
Solids granular viscosity μ_s and conductivity κ_s :

$$\mu_s = \frac{\mu}{\eta g_0}\left[1+1.6\eta g_0 \varepsilon_s\right]^2 + 0.6\mu_b \qquad [5]$$

where dilute viscosity is: $\mu = \frac{5\sqrt{\pi}}{96}\rho_s d_p \sqrt{\Theta_s}$ and bulk viscosity: $\mu_b = \frac{8}{3\sqrt{\pi}}\rho_s d_p \varepsilon_s^2 g_0 \eta \sqrt{\Theta_s}$ and the radial distribution function: $g_0 = \frac{1}{\varepsilon_g} + 1.5\frac{\varepsilon_s}{\varepsilon_g^2} + 0.5\frac{\varepsilon_s^2}{\varepsilon_g^3}$ and $\eta = \frac{1+e}{2}$, $\varepsilon_g = 1-\varepsilon_s$.

$$\kappa_s = \frac{\kappa}{\eta g_0}\left[1+2.4\eta g_0 \varepsilon_s\right]^2 + 1.5\mu_b \qquad [6]$$

Where dilute granular conductivity is: $\kappa = \frac{75\sqrt{\pi}}{96}\rho_s d_p \sqrt{\Theta_s}$.
Solids granular pressure is defined as:

$$P_s = \rho_s \varepsilon_s \left(1+4\eta g_0 \varepsilon_s\right)\Theta_s \qquad [7]$$

The collisional dissipation of granular energy is defined as:

$$J_s = \frac{12}{\sqrt{\pi} d_p}\varepsilon_s^2 g_0\, \Theta_s^{1.5} \qquad [8]$$

The only constitutive relation used in this study that was not derived from kinetic theory is the gas/solids friction coefficient (β). We use in this study the well-known Wen and Yu correlation:

$$\beta = \frac{3}{4}C_D \frac{\rho_g \varepsilon_g \varepsilon_s \left|\mathbf{u}_g - \mathbf{u}_s\right|}{d_p}\varepsilon_g^{-2.65} \qquad [9]$$

Where $C_D = \begin{cases} 24/\mathrm{Re}\left(1+0.15\mathrm{Re}^{0.687}\right) & \mathrm{Re} < 1000 \\ 0.44 & \mathrm{Re} \geq 1000 \end{cases}$ and $\mathrm{Re} = \frac{\rho_g \varepsilon_g \left|\mathbf{u}_g - \mathbf{u}_s\right| d_p}{\mu_g}$.

Time-averaged constitutive relations

All constitutive relations presented in the previous section are non-linear, and thus, must be time-averaged. A Taylor series expansion about the mean is conducted for all the constitutive relations.

Whether such series converge or not and how many terms are needed to express the non-linear constitutive relations are the subjects of this section.
The first example of a constitutive relation derived from KTGF is the collisional dissipation term. The time averaging of this term has been analyzed by Hrenya and Sinclair (1997) who gave this expression:

$$\bar{J}_s = \frac{12}{\sqrt{\pi} d_p} \overline{\varepsilon_s^2 g_0 \, \Theta_s^{1.5}} = \frac{12}{\sqrt{\pi} d_p} \overline{f_1(\varepsilon_s) f_2(\Theta_s)} \approx \frac{12}{\sqrt{\pi} d_p} \left[f_1(\bar{\varepsilon}_s) f_2(\bar{\Theta}_s) + f_1^{\varepsilon} f_2^{\Theta} \, \overline{\varepsilon_s' \Theta_s'} \right] \qquad [10]$$

Where $f_1^{\varepsilon} = \left(\frac{\partial f_1}{\partial \varepsilon_s} \right)_{\bar{\varepsilon}_s}$ and $f_2^{\Theta} = \left(\frac{\partial f_2}{\partial \Theta_s} \right)_{\bar{\Theta}_s}$.

Recognizing the separation of variables in the collisional dissipation term, equation (10) is just a Taylor series expansion that only includes the 0th and 1st order terms. Stopping the series expansion at the 1st term can only be motivated by small fluctuations in the flow variables. However, we have seen in Figure 1 that large oscillations are computed by the transient model, and thus, such a limited expansion may not be valid.
To show that such Taylor expansion may not even converge, let's take a simple example of the function $\bar{f}_2(\Theta_s)$ and expand it about the mean:

$$\bar{f}_2(\Theta_s) = \underbrace{\underbrace{\underbrace{f_2(\bar{\Theta}_s)}_{term\,1} + \underbrace{f_2^{\Theta} \overline{\Theta_s'}}_{=\,zero}}_{term\,2} + \frac{1}{2!} f_2^{2\Theta} \overline{\Theta_s'^2}}_{term\,3} + \frac{1}{3!} f_2^{3\Theta} \overline{\Theta_s'^3} + \underbrace{\frac{1}{4!} f_2^{4\Theta} \overline{\Theta_s'^4} + \ldots}_{term\,4} \qquad [11]$$

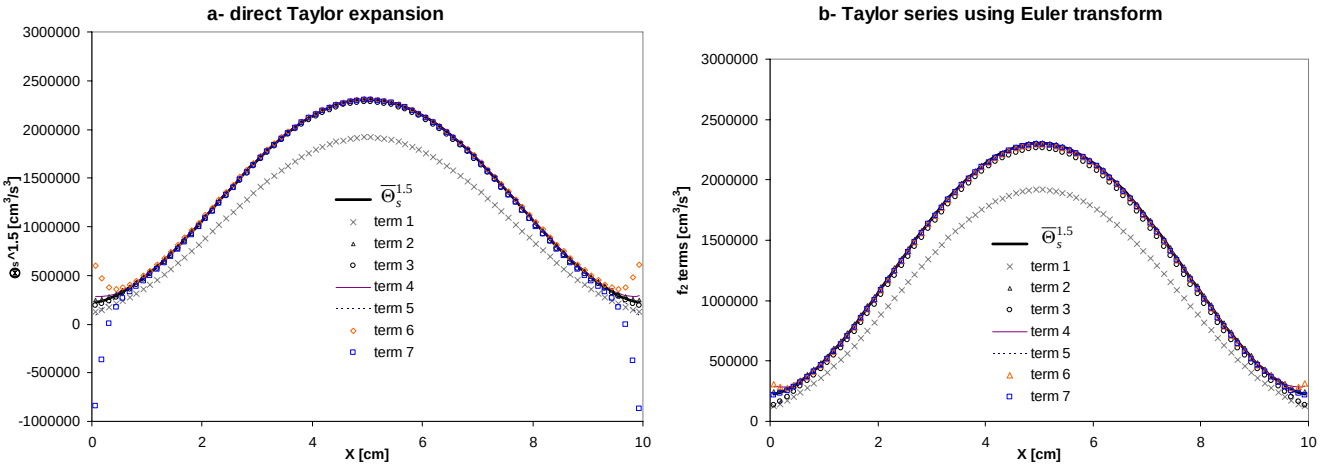

Figure 2 The diverging Taylor series expansion is made to converge using the Euler transformation.

Because of the large amplitude of oscillations in the granular temperature, the Taylor series expansion of function f_2 diverges for the high order terms. After recognizing that terms in the Taylor series expansion alternatively change sign, the Euler transformation was used (See numerical recipes) when the high order terms start diverging. Figure 2-b shows that a good convergence is achieved with the Euler transformation. Figure 2-a shows that the Taylor series expansion diverges when using high order terms, but does not show the need for taking higher order terms since using up to term 2 seems to fit the function f_2

reasonably well. So we turn our attention to our original problem of expanding the function $f_1 f_2$ about mean values:

$$\bar{f}_1(\varepsilon_s)\bar{f}_2(\Theta_s) = \underbrace{\underbrace{f_1(\bar{\varepsilon}_s)f_2(\overline{\Theta}_s)}_{term1} + f_1^{\varepsilon} f_2^{\Theta}\,\overline{\varepsilon'_s\Theta'}_s}_{term\ 2} + \underbrace{\frac{1}{2!}\left(f_1 f_2^{2\Theta}\,\overline{\Theta'^2_s} + f_1^{2\varepsilon} f_2\,\overline{\varepsilon'^2_s} + f_1^{\varepsilon} f_2^{2\Theta}\,\overline{\varepsilon'_s\Theta'^2_s} + f_1^{2\varepsilon} f_2^{\Theta}\,\overline{\varepsilon'^2_s\Theta'_s} + f_1^{2\varepsilon} f_2^{2\Theta}\,\overline{\varepsilon'^2_s\Theta'^2_s}\right) + \ldots}_{term\ 3} \qquad [12]$$

Where, for e.g., $f_2^{2\Theta} = \left(\frac{\partial^2 f_2}{\partial \Theta_s^{\,2}}\right)_{\overline{\Theta}_s}$. All derivatives were derived analytically using Maxima 5.9.2 software (http://maxima.sourceforge.net).

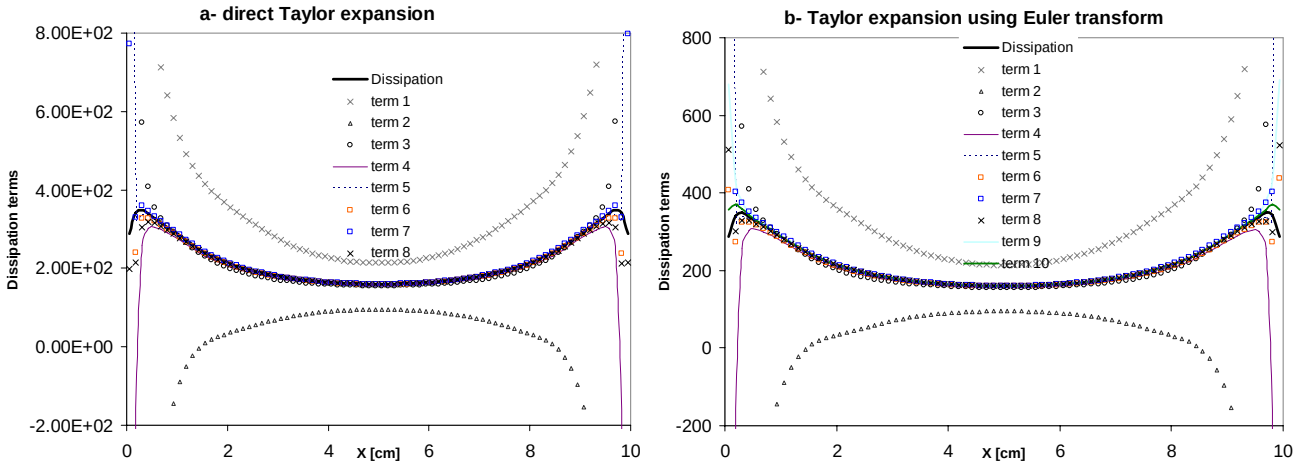

Figure 3 Convergence behavior of the Taylor series expansion of the dissipation terms with and without Euler transformation.

In Figure 3, Euler transformation is implemented for the 5th and higher terms where we observed an increase, or divergence, in the magnitude of the terms. It is noteworthy mentioning that term 2 or the expansion used in equation (10) is not a satisfactory representation of the time averaged collisional dissipation. We had to continue the expansion to the 10th term using Euler transformation in order to obtain a reasonably converged series expansion. The previous study of Hrenya and Sinclair assumed the same form for the dissipation as equation (10) due to the assumption of small fluctuations. However, this study proves that such an assumption is not reasonable. Also Figure 3 shows that most of the disagreement in the Taylor series expansion occurs near the walls because the largest fluctuations in volume fractions are near the walls where dense clusters form (see figure 1-a).

A similar behavior is observed for the Taylor series expansion of solids viscosity where the Euler transform is required to obtain a converged series. Here again, Euler's technique makes this diverging series to converge because of the alternating sign of the series terms. It is clear from Figure 4 that the "laminar" viscosity $\mu_s\left(\bar{\varepsilon}_s, \overline{\Theta}_s\right)$ or term 1 in Taylor series expansion will overpredict the time-averaged viscosity and so other terms in the Taylor series expansion must be considered.

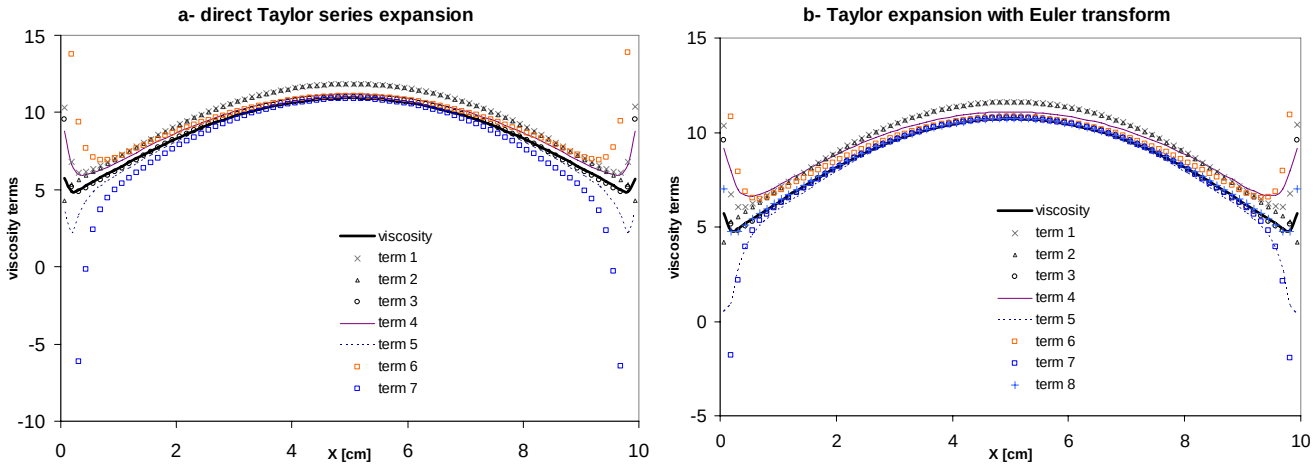

Figure 4 Convergence behavior of the Taylor series expansion of the solids viscosity terms with and without Euler transformation.

The effect of solids viscosity in the vertical momentum equation is introduced as $\overline{\mu_s \frac{\partial v_s}{\partial x}}$, so that it's not enough to obtain just the values of $\overline{\mu}_s$. We approximate the time-averaged shear stress in the following manner:

$$\overline{\mu_s \frac{\partial v_s}{\partial x}} = \overline{\mu_s \frac{\partial \left(\overline{v}_s + v_s'\right)}{\partial x}} \qquad [13]$$

In equation (13), we make use of the Taylor series expansion already developed for $\overline{\mu}_s$, and each of these terms will be multiplied by the instantaneous and averaged velocity gradient, which doubles the number of terms (or correlations) in the original series for $\overline{\mu}_s$.

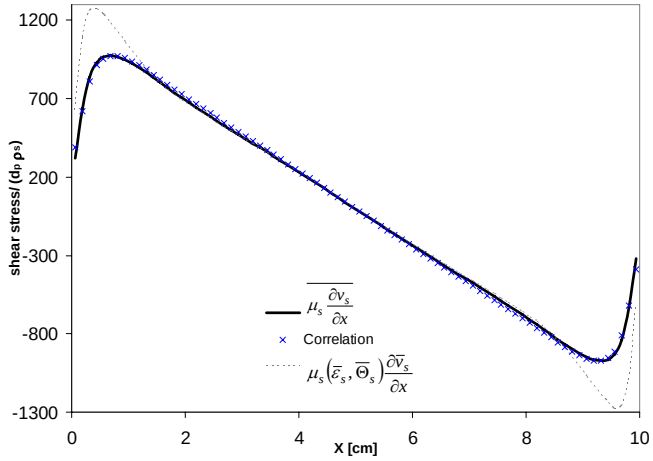

Figure 5 Comparison between time-averaged shear stress and the correlation

Figure 5 shows the "laminar" or steady shear and the "turbulent" or time-averaged shear stress results are similar in the middle of the channel except near the walls where large differences occur. It's clear that

correlations of fluctuating volume fraction, granular temperature and gradient of solids velocity cannot be neglected. It is remarkable that the effect of the non-linearity of the shear stress term is noticeable before even mentioning the contribution of Reynolds-like terms that rise from the time-averaging of the convective terms. However, we'll address the importance of the shear stress later in this section when we show the Reynolds stresses results.

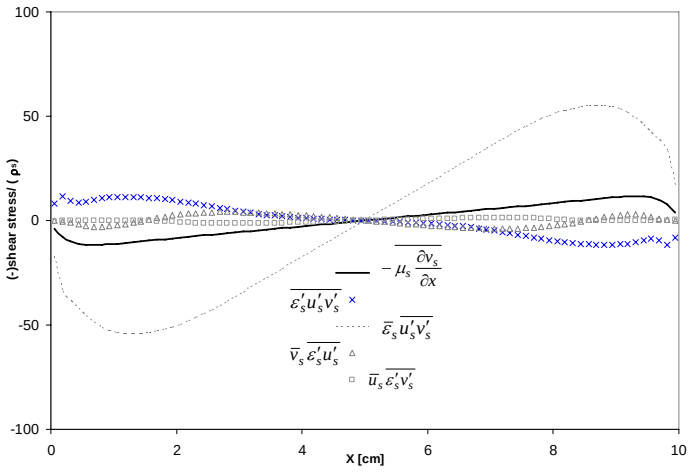

Figure 6 Comparison between different Reynolds-like stresses and time-averaged shear stress

It is clear from Figure 6 that the major contribution to the shear stresses will be from the traditional Reynolds stress $\overline{\varepsilon}_s \overline{u_s' v_s'}$. The contribution of the triple correlation $\overline{\varepsilon_s' u_s' v_s'}$ has opposite sign (may contribute to a negative turbulent viscosity) and is comparable in magnitude to the time-averaged shear stress. The smallest contribution to the turbulent stresses is due to $\overline{u}_s \overline{\varepsilon_s' v_s'}$ because the average of the radial velocity is negligible.

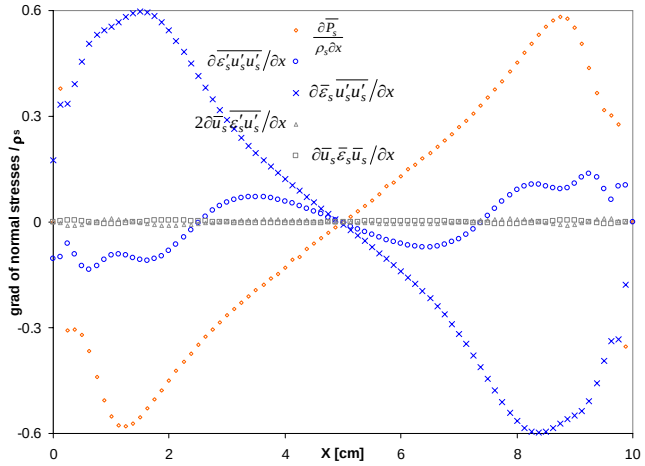

Figure 7 Comparison between different normal Reynolds stresses and time-averaged solids pressure

Figure 7 shows the gradients of time-averaged solids pressure and normal Reynolds stresses. Again, all terms involving $\overline{u}_s$ are negligible and the most important terms are due to gradients of solids pressure and

normal stress $\partial\bar{\varepsilon}_s\overline{u_s'u_s'}/\partial x$. This is quite different from the analysis of the shear stresses where the time-averaged shear stress was not as significant.
The solids pressure is not a linear function of solids volume fraction, but is a linear function of granular temperature. However, the time-averaged solids pressure must be correlated in a similar manner as in equation (12). The results of the Taylor series expansion are presented in Figure 8. Note that in this case we did not need to use the Euler transformation since this series converged because of the linear dependence of solids pressure on the granular temperature. It is clear from figure 8 that using the steady-state values (1st term) or even the second term in Taylor series expansion (2nd term) will significantly reduce the ability of a reduce model to accurately represent the time-averaged solution.

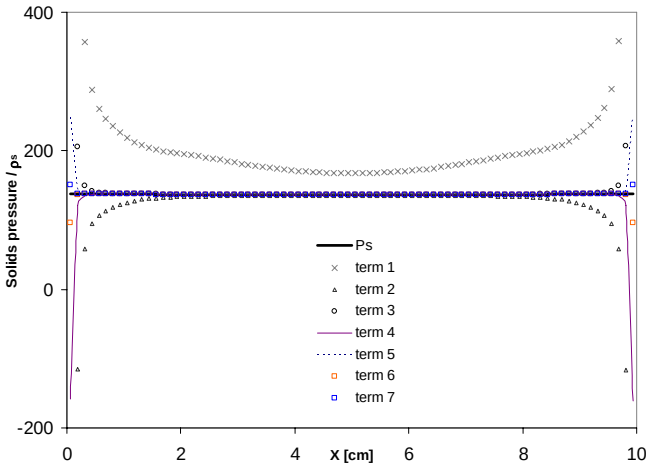

Figure 8 Normal Taylor series expansion of time-averaged solids pressure

We have shown at the beguiling of this section the importance of correctly expanding the dissipation of granular energy (see figure 3). Let's now focus our attention on the production due to shear of granular energy: $\overline{\mu_s \frac{\partial v_s}{\partial x}\frac{\partial v_s}{\partial x}}$.

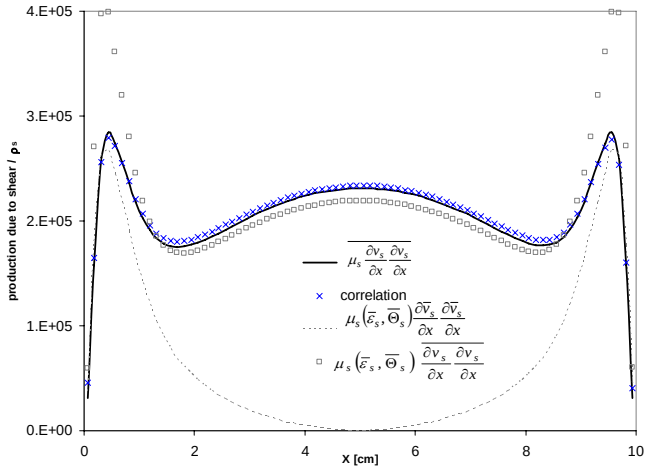

Figure 9 Comparison between time-averaged and "laminar" (or first term in Taylor series expansion) production of granular energy

to 7th

production of granular energy. The laminar expression, or 0th term in the Taylor expansion, fails to capture the significant production of granular energy at the center of the channel because the time-averaged velocity gradient is zero at that location. Figure 9 shows that properly correlating the term: $\overline{\frac{\partial v_s}{\partial x}\frac{\partial v_s}{\partial x}} = \frac{\partial \bar{v}_s}{\partial x}\frac{\partial \bar{v}_s}{\partial x} + \overline{\frac{\partial v_s'}{\partial x}\frac{\partial v_s'}{\partial x}}$ is not enough as the production is underpredicted at the center of the channel and an overshoot near the walls is exaggerated due to the approximation of laminar solids viscosity as was seen previously during the study of the shear stress (see Figure 5).
Other terms arising from the time-averaging of the granular temperature equation (see equation 4) such as granular conductivity and convection terms will be ignored and we will demonstrate later that properly correlating the production and dissipation of granular energy is sufficient.
Let's turn our attention to terms that do not arise from kinetic theory of granular flows such as $\bar{I}_{gsy}$ and $\overline{\varepsilon_s \frac{\partial P_g}{\partial y}}$. First, the solids volume fraction and axial pressure gradient are not correlated as shown in Figure 10, and thus the following equality is satisfied:

$$\overline{\varepsilon_s \frac{\partial P_g}{\partial y}} = \bar{\varepsilon}_s \frac{\partial \bar{P}_g}{\partial y} + \overline{\varepsilon_s' \frac{\partial P_g'}{\partial y}} \cong \bar{\varepsilon}_s \frac{\partial \bar{P}_g}{\partial y} \qquad [14]$$

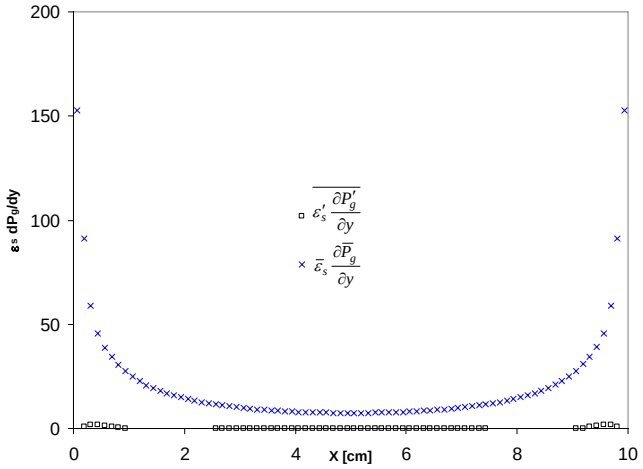

Figure 10 Verification that the solids volume fraction and gas pressure gradient are not correlated

Now, let's focus on the gas/solids momentum exchange $\bar{I}_{gsy}$, which many would argue is one of the most important terms in the momentum equations. Let's first assume that the momentum exchange term is less important in the horizontal direction, so that we can focus on deriving an expansion of the $\bar{I}_{gsy}$ term in the vertical direction only, which yields: $-\bar{I}_{gsy} = \overline{\beta(v_g - v_s)}$. If we assume that the magnitude of the relative velocity is equal to the absolute value of the vertical component of the relative velocity, then we can show that equation (9) reduces to:

$$-\bar{I}_{gsy} = 18\mu_g \frac{\overline{(1-\varepsilon_g)}}{(\varepsilon_g^{2.65} d_p^2)} V_r \left(0.15|V_r|^{0.687}(\varepsilon_g \rho_g d_p/\mu_g)^{0.687} + 1\right) \qquad [15]$$

Here we note that $V_r = v_g - v_s$, which shows less that 0.1% error in computing equation (15) as compared with using the magnitude of relative velocity instead. Also there is no loss of accuracy in assuming that the Re number is always less than 1000 in this study so that C_D is formulated using only one expression. Since in equation (15), one would recognize that it is not possible to separate the volume fraction and relative velocity as was done in equation (12), so that equation 15 needs to be expanded in a Taylor series of two variables (see for e.g. Greenberg, 1998, page 638). In general we can express the Taylor series as:

$$-\bar{I}_{gsy} = f\left(\varepsilon_g, V_r\right) = \sum_{j=1}^{\infty}\left\{\frac{1}{j!}\left(\varepsilon_g' \frac{\partial}{\partial \varepsilon_g} + V_r' \frac{\partial}{\partial V_r}\right)^j f\left(\bar{\varepsilon}_g, \bar{V}_r\right)\right\}$$

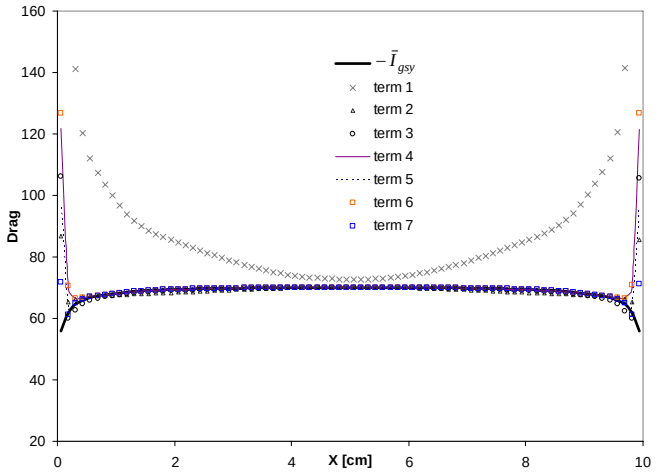

Figure 11 Convergence check on the Taylor series expansion of momentum exchange force

Figure 11 shows that a Taylor series expansion of the function of two variables eventually converges without a need of using Euler transformation. Again, the laminar, or first term, fails to predict the qualitative behavior of the time-averaged function and higher order terms have difficulty capturing the large oscillations and coupling of void fraction and solids velocity near the walls. Another difficulty is the large amount of computer code generated by the derivatives used in the correlations; for the gas/solids drag (up to the 7^{th} term), for e.g., uses about 1000 line of Fortran code (derivatives for viscosity formulation use a bit more than that). Furthermore, the large amount of correlations generated from time-averaging governing equations makes this approach impractical, although possible as shown in this study. Definitely, more research is needed in multiphase flow turbulence modeling in order to produce ROM with similar accuracy as in single-phase flow (e.g. k-epsilon model).

Steady-state results

Steady-state results are obtained by adding to the governing equations the correlations derived in the previous section of this study. We still used the transient terms in the governing equations and started the simulation from a uniform (flat horizontal profiles were used) initial state where solids volume fraction was set to 0.03, solids and gas vertical velocities were set to 5.2 and 5.5 respectively, granular temperature was set to 1 m^2/s^2 and finally zero horizontal gas and solids velocities. The transient simulation converged to a steady-state after few seconds of simulation. The results reported here were obtained after 10 sec of

simulation. We compare the steady results with time-averaged results obtained without using a time-averaged model, so that no correlations were used.

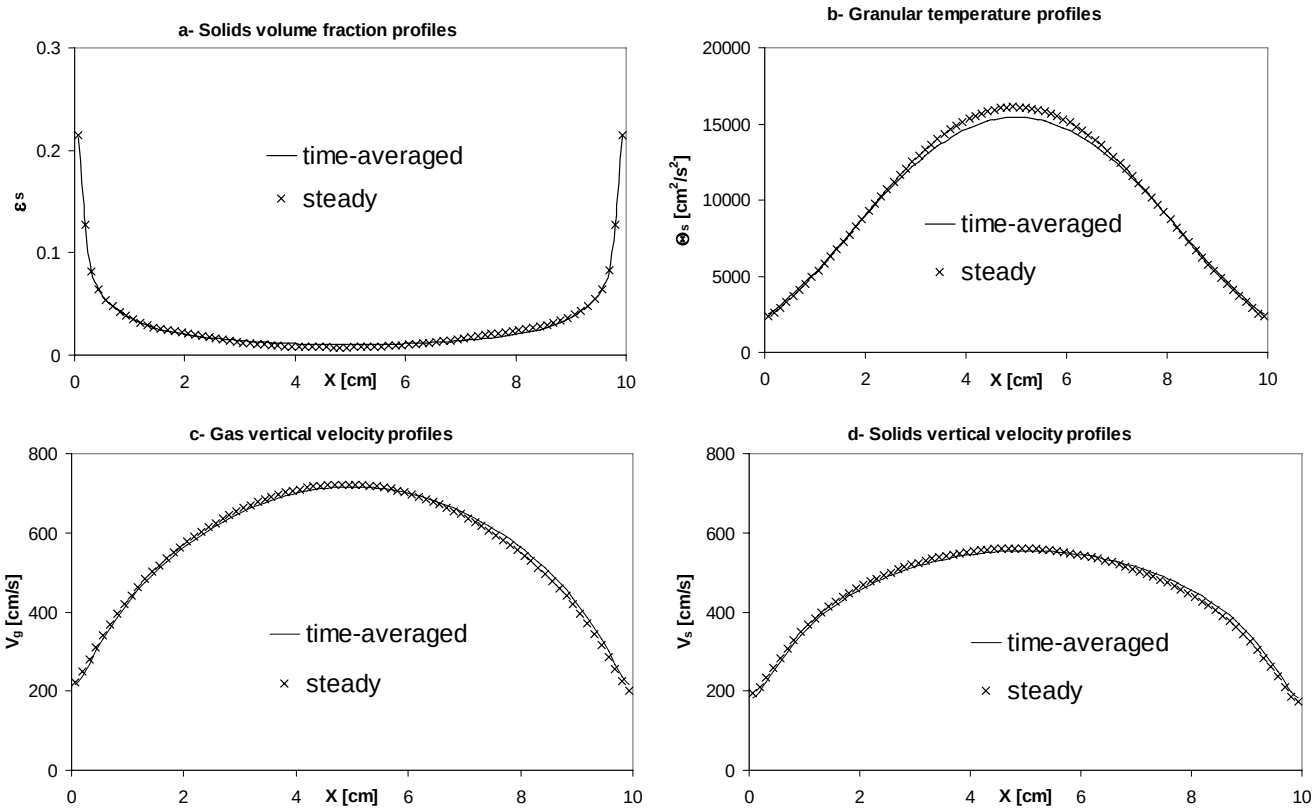

Figure 12 Comparison of time-averaged and steady-state results using all correlations arising from time-averaging non-linear terms in solids momentum and granular energy equations.

Figure 12 shows good comparison of time-averaged transient results and steady-state results obtained by using all correlations presented in this study. It took only few minutes of CPU time to compute the steady results shown in Figure 12. In contrast, it took about 6 hours of CPU time to compute 70 sec of simulation needed to obtain the time-averaged results presented in Figure 12. This figure also shows that the granular temperature was slightly over-predicted at the center of the channel mainly due to a higher production of granular energy as seen in Figure 9, which also caused the solids volume fraction to be slightly under-predicted at the center of the channel. We should mention that some non-linear terms were not accounted for (without much loss of accuracy) in the steady model, namely all the correlations from the gas momentum equation, conductivity and convection terms in the granular energy equation, as well as gas/solids drag term in the solids horizontal momentum equation.

Conclusions

We demonstrated in this study that it is possible to obtained steady-state results that match the time-averaged computational results of a transient model. However, such a model seems impractical because of the large number of correlations that need to be modeled. This study demonstrates that large oscillations are computed in gas/solids flows that require a large number of correlations when non-linear terms were expanded using Taylor series.

Nomenclature

d_p: particle diameter.

e: particle-particle restitution coefficient.

g_i : acceleration of gravity in the i direction.

g_0 : radial distribution function at contact.

I_{nm}: momentum exchange.

J_s: granular energy dissipation due to inelastic collisions.

P_m: pressure of phase m.

S_{mij}: mean strain-rate tensor.

U_m: averaged velocity of phase m.

Greek letters:

β, β_{gs}: gas/solids friction coefficient.

ε_m: volume fraction of phase m.

η: constant depending on particle restitution coefficient equal to $(1+e)/2$.

κ: solids phase dilute granular conductivity.

κ_s: conductivity of solids granular energy.

μ: solids phase dilute granular viscosity.

μ_b: bulk viscosity of the solids phase.

μ_g^t: turbulent eddy viscosity for gas phase.

Π: turbulence exchange terms between gas and solids phases.

Θ_s: granular temperature.

ρ_m: density of phase m.

τ_{mij} : stress tensor of phase m.

Indices:

g: gas phase.
i, j: indices used to represent spatial direction and in Einstein summation convention.
m: phase m: g for gas and s for solids phases.
max: maximum packing.
s, p: solids or particulate phase.

References

Press WH, Teukolsky SA, Vetterling WT, Flannery BP, Numerical recipes in Fortran 77, 2006. Cambridge Univ. Press, NY.
Greenberg MD, Advanced engineering mathematics, 1998. Prentice Hall NJ.
Hrenya CM, Sinclair JL. AIChE J. 1997;42:853-869.
Gidaspow D. Multiphase flow and fluidization: continuum and kinetic theory description. San Diego: Academic Press, 1994.
Lun CKK, Savage SB, Jeffrey DJ, Chepurniy N. J Fluid Mech. 1984;140:223-256.
Benyahia S, Syamlal M, O'Brien TJ. AIChE J. 2007; 53:10, DOI 10.1002/aic.11276.